UCID--20052

DE84 010921

SEM STUDIES OF STRESSED AND IRRADIATED CLIMAX STOCK QUARTZ MONZONITE

J. M. Beiriger
W.B. Durham

February, 1984

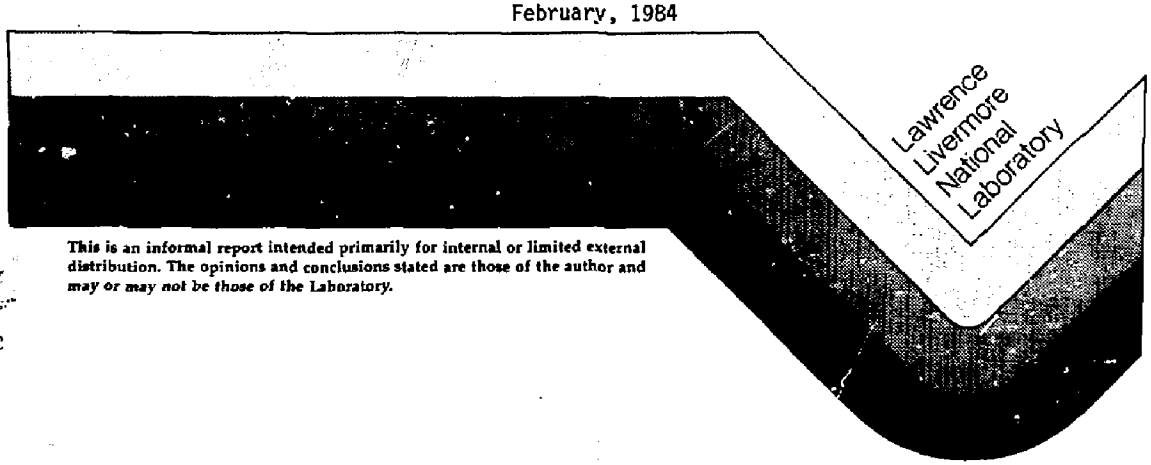

SEM STUDIES OF STRESSED AND IRRADIATED CLIMAX STOCK QUARTZ MONZONITE*

J. M. Beiriger and W. B. Durham

ABSTRACT

In an effort to find the mechanism by which gamma irradiation weakens the unconfined compressive strength of Climax Stock quartz monzonite (CSQM), sections of rock which had been irradiated and loaded to near failure were studied by scanning electron microscopy and compared to sections of rock which had been loaded but not irradiated. The quantities measured and compared were numbers and lengths of microfractures in the rock. We found that the crack parameters depended neither on irradiation treatment nor even on stress history, except in one sample which actually failed. By comparison to cracks counted in other granites by other workers, the crack statistics on CSQM are much noisier and much less indicative of stress history. CSQM is structurally more heterogeneous than the other granites, which is probably the cause of the greater noise level.

*This work was performed under the auspices of the U.S. Department of Energy by the Lawrence Livermore National Laboratory under contract W-7405-ENG-48. This study was conducted as part of the Nevada Nuclear Waste Storage Investigations of the U.S. Department of Energy.

2697x/0115x

INTRODUCTION

In an exploratory experiment Durham (1982) found that massive doses of gamma irradiation apparently degraded the unconfined compressive strength of Climax Stock quartz monzonite (CSQM) by approximately 20%. Since the Climax Stock has recently housed an experimental nuclear waste storage facility, known as the Spent Fuel Test-Climax (SFT-C) (Ramspott et al. 1979), there is some interest in establishing the veracity and understanding the cause of this degrading effect. Accepting that brittle failure in rocks is intimately related to the creation and growth of microfractures, a difference in the failure strength of two rock populations might be expected to be reflected in the pre-failure characteristics of the microstructure of the rocks. In this study, we test this expectation by measuring the crack density of irradiated and non-irradiated CSQM which has been loaded to > 90% of the mean failure strength of the irradiated material. There is strong evidence that in granitic rocks loaded to such levels in both the confined and unconfined situations, microfractures which are visible to the scanning electron microscope (SEM) will begin to form even though the rock has not ultimately failed (Sprunt and Brace, 1974; Hadley, 1976; Tapponnier and Brace, 1976; Kranz, 1979; Sano et al., 1981). If the failure strength of CSQM is lowered 20% by gamma irradiation, then one would expect that following the loading treatment the irradiated rock will have a higher crack density than the non-irradiated rock.

PROCEDURES

Ten test cylinders of CSQM measuring 25.4 mm in diameter and 63.5 mm in length were prepared in the same manner as the earlier samples (Durham, 1982). The ends of the cylinders were ground flat and were parallel to ± 0.08 mm, compared with ± 0.005 mm in the case of the earlier samples. The source of the material was a 152-mm-diameter core from hole U15.01-TCH# 1 taken horizontally into the mine wall near the site of SFT-C. Note that the material used in the earlier study came from the site of Heater Test 1, roughly 75 m away at the same horizontal level.

Five of the samples were gamma-irradiated and five samples were held for control. The treatment of the two groups was kept as similar as possible to that of analogous groups in the earlier study. The total dose to the irradiated samples was approximately 10 MGy (10^9 rads) or roughly six times the maximum total dose to rock at SFT-C.

The mechanical testing hardware and its arrangement in the column was the same as in the tests conducted by Durham (1982) approximately seven to eight months earlier, except that the displacement of the loading piston was halted when the compressional stress on the samples reached 150 ± 1 MPa. Once at 150 MPa, the piston position was held constant for 60 s, during which time the load did not change within the 1 MPa resolution of the data record. After 60 s the load was released. The ten samples were tested in an alternating sequence: non-irradiated, irradiated, non-irradiated, etc. None of the ten samples failed in the tests, an improbable result given that five of the samples had strengths of 164 ± 35 MPa (1 s.d.), based on the earlier study. (The most probable result was that one or two of the five irradiated samples

would fail.) Therefore, the test was repeated on two samples from each group, with the maximum load increased to 180 MPa. This time one sample from each group failed, one of them (non-irradiated) as a result of an accidental rapid overloading which demolished the sample. Table 1 summarizes the results.

SEM sections were cut perpendicular to the cylinder axis at approximately the mid-plane of each sample. Presumably, the cracks which developed under load were predominantly "vertical", i.e. with normals perpendicular to the loading direction, (Tapponier and Brace, 1976) so the "horizontal" section thus sampled should provide the best view of these cracks.

The preparation technique for the SEM specimens was the same as that described by Weed and Durham (1982). Fresh cracks in the samples were counted from SEM photographs by the method outlined in Weed and Durham (1982). Fresh and old cracks were distinguished on the basis of the criteria defined by Weed and Durham (1982). The SEM photomicrography was conducted in two phases. In the first phase, one diametrical traverse (called pass A) was taken on each section using the same detector, signal (a mix of backscattered, BSE, and secondary electrons, SE), and specimen tilt angle (30^{o}) as Weed and Durham used. In the second phase, two additional traverses (called passes B and C) were made on each section parallel to and 2 mm on either side of the original traverse. The detector used in the second phase was a recently acquired solid-state backscattered electron quadrupole detector that has a much greater collection efficiency for BSE and therefore reveals cracks in better contrast. In the second phase, therefore, the signal observed was based solely on reflected electrons from the incident beam and the section was oriented at a 0^{o} angle of tilt, normal to the incident electron beam. Hereafter, we will refer to the signals used in the first and second phases as BSE/SE and BSE, respectively. The two types of images are compared in Figures 1 and 2.

OBSERVATIONS AND DISCUSSION

Presentation of Results. Table 2 gives the results for Young's modulus (E) for the ten runs. Note the good agreement of repeat measurements on samples 1-4. The range of values of E_1 and E_2 (defined in Table 2) is approximately the same as found on earlier samples by Durham (1982). Therefore we can conclude that the calibration of the load on the sample did not change significantly from the earlier study. In particular, we can be confident that the lower load (nominally 150 MPa) applied to the ten samples tested here was approximately 90% and 75%, respectively, of the mean strengths of irradiated and non-irradiated samples as measured by Durham (1982).

Results of the crack counting are given by sample in Table 3 and by radiation/stress treatment in Table 4. The crack parameters listed are the same as those in Weed and Durham (1982): number of fresh cracks observed per unit area, average length of fresh cracks, and average total length per unit area of fresh cracks. Results in both tables are broken down by pass. In pass A, a total of 482 fresh cracks were identified in 80 micrographs; in pass B, 236 in 59 micrographs; and in pass C, 272 in 68 micrographs. The total surface area of rock photographed and quantified was about 8 mm^2. Crack counting results are also given in Table 4 for a virgin sample from the center of a 150-mm diameter core taken along side a canister emplacement hole at SFT-C. It has been examined previously for cracks, being the least disturbed of the six samples examined by Weed and Durham (1982), so also provides a study-to-study comparison of results. Crack counting results for this sample from the Weed and Durham study also are given in Table 4. Raw data for individual cracks are available from the authors.

The results show a great deal of noise and a dependence of crack counting statistics upon which detector was used in the SEM, but do not reveal any difference between irradiated and non-irradiated rock. The remainder of the discussion centers on these points.

BSE/SE vs BSE. The BSE/SE signal in the SEM apparently reveals more cracks than the BSE signal (Tables 3 and 4). The cracks so revealed in BSE/SE, however, are on average less than half as long as those revealed in BSE, resulting in an average total length of crack per unit area that is slightly greater in BSE. The difference is unmistakable, but since we have not made comparisons of the two techniques on the same area of rock, and since the rock is so inhomogeneous, we can only hypothesize as to the cause of the difference. (Note that a valid point-by-point comparison of the two techniques may not be possible because of the judgmental role played by the operator. Having viewed and counted an area in BSE/SE, he or she may retain a bias in counting the same area in BSE.) SE do typically provide better areal resolution than BSE because of the physics of electron interaction with surfaces, so the BSE signal may not be resolving the shorter, narrower cracks. Another possible explanation is related to the intentional exclusion of grain boundary cracks from this study. The BSE signal is much more sensitive to chemistry than BSE/SE (compare Figures 1 and 2), so that grain boundaries, and cracks which lie along them, are more obvious in BSE. Therefore, some of the cracks counted in pass A may have been grain boundary cracks that were mistakenly identified.

Noise. The earlier study by Weed and Durham (1982) identified the high level of noise inherent in crack statistics in CSQM; the high noise persists in the present study. For example, calculated standard deviations based on normal

distributions for many of the three crack parameters are typically as large as the means of those parameters (see example in Table 5). By the comparison illustrated in Table 5, standard deviations for crack density in Westerly granite are typically less than half the mean values (Tapponnier and Brace, 1976) and for crack length in Barre granite are about 60% of the mean values (Kranz, 1979).

A more meaningful, though less quantitative, measure of noise comes from classifying the data by pass for a given sample. Passes B and C were essentially identical in technique, operator, time taken, etc., differing only in that they were 4 mm apart, yet give crack densities across a given sample which can vary by as much as a factor of two (Table 3). While systematic limitations exist with the technique, as discussed in the next paragraph, the cause here is clearly inhomogeneity of the rock. Petrographically, CSQM is strongly heterogeneous on the millimeter size scale (Fig. 3). Most of the rock is composed of grain sizes ranging from 0.25 to 2 mm, but the rock is populated irregularly by quartz phenocrysts (about 10% by volume) typically 5 mm across and by potassium feldspar phenocrysts (about 5% by volume) up to 150 mm long. Westerly granite, on the other hand, is finer-grained (0.25 to 1 mm) and petrographically more uniform than CSQM and as a result may be less prone to noise in crack distributions (Table 5). Comparison of unconfined failure strength statistics for CSQM and other granites is striking. For Westerly the unconfined failure strength is 230 $\pm$ 10 MPa (Byerlee, 1969). Kranz and Scholz (1977) indicate that the unconfined strength of Barre granite is 220 $\pm$ 10 MPa (although they give no raw data). The scatter in unconfined strength of Oshima granite is clearly less than $\pm$ 5% based on eight test results published by Sano et al. (1981). For unirradiated, unconfined CSQM, the failure strength is 204 $\pm$ 33 MPa, based on 12 measurements by Durham (1982).

Stressed vs. Unstressed Rock. The question arises as to whether or not we are able to resolve in the crack structure any manifestation of the loading treatment. The crack statistics for the single BSE pass on the virgin rock (Table 4) compare as follows to those for the 18 BSE passes on stressed rock (Tables 3, 4): The 91 cracks/mm^2 in the virgin rock is 20% below the mean for all the stressed CSQM but ranks eleventh from the top (i.e. only one below median) when all 19 passes are compared. The average length per crack in the virgin is 10% more than the mean for all stressed CSQM and ranks sixth (in a tie) among the 19 passes. Incipient failure in other granites seems to be marked by increased number densities and increased lengths of cracks (Table 5). It appears that we cannot resolve any significant microstructural difference between stressed and unstressed CSQM. Remarkably, even Sample 2, the one sample that failed under 180 MPa load, showed an unusual crack length (52 μm) only in one of the three SEM passes. The statistics from the other two passes on Sample 2 reveal no evidence of the failure.

The damage we imparted by loading the CSQM should have been profound. Admittedly our knowledge of the failure strength (σ_f) is not well resolved, but it appears unlikely that σ_f > 205 MPa for "typical" untreated CSQM at 1 atmosphere confining pressure, based on all 136 measurements of σ_f made by Durham (1982) and Durham et al. (1983). Therefore, a load corresponding therefore to no less than 0.88 σ_f (i.e., 180 MPa) was applied to three of the nine samples studied here by SEM. Except in one pass on Sample 2 those three were indistinguishable from the six loaded only to 150 MPa and from the one unstressed sample. By comparison (Table 5), Tapponier and Brace (1976) saw a significant increase in crack density at stresses as low as .58 σ_f and Kranz (1979) found that unconfined Barre

granite at $\sigma = .87\ \sigma_f$ is unmistakably more cracked than the virgin material. It appears, therefore, that crack generation at given levels of σ/σ_f is retarded in CSQM with respect to that in Westerly and Barre granites. Noisy crack data in CSQM make a quantitative statement difficult, but CSQM appears to show no microscopic crack damage up to at least $0.9\ \sigma_f$.

It is unlikely that the difference between CSQM and other granites is an artifact of technique. Surface preparation techniques for all studies compared here have essentially duplicated the grinding/polishing/ion-milling sequence developed by Brace et al. (1972). SEM was used for observation in all studies and most "counting" micrographs were taken at 300-500x magnification (only Sprunt and Brace (1974) counted at higher magnification). Practical SEM resolution limits are comparable in all studies.

CONCLUSIONS

The experimental data of this study provide no support for the hypothesis that stressed, irradiated CSQM is more cracked than stressed, non-irradiated CSQM, either at stress difference (σ) = 150 MPa (lines 3 and 4 of Table 4), σ = 180 MPa (lines 1 and 2), or with combined statistics (lines 5 and 6). The lack of difference is not necessarily due to the lack of an effect of gamma irradiation on unconfined strength, however, since the CSQM stressed below failure in this study, irradiated or otherwise, does not show a measurable change in its crack structure with respect to unstressed CSQM. If the effect of gamma irradiation on failure strength (σ_f) is real, it will not be observed in the microcrack structure unless samples are loaded to even higher levels than used here. Such an experiment is probably not practical

for two reasons: 1) initiation of incipient failure (i.e. microfracturing) in CSQM apparently occurs only at stresses very close to σ_f, and σ_f in any given sample is known only to ± 15%; and 2) inherent noise levels of crack parameters in CSQM are very high. Underlying both problems is a common factor: the considerable structural inhomogeneity of CSQM.

REFERENCES

Brace, W. F., E. Silver, K. Hadley, and C. Goetze, Cracks and pores: A closer look, Science, 178, 162-164, 1972.

Byerlee, J. D., Reply, J. Geophys. Res., 74, 5349-5350, 1969.

Costantino, M. S., Statistical variation in stress-volumetric strain behavior of Westerly granite, Int. J. Rock Mech. Min. Sci., 15, 105-111, 1978.

Durham, W. B., The effect of gamma irradiation on the strength of Climax Stock quartz monzonite, LLNL Report UCRL-87475, 1982.

Hadley, K., Comparison of calculated and observed crack densities and seismic velocities in Westerly granite, J. Geophys. Res., 81, 3484-3494, 1976.

Kranz, R. L., Crack growth and development during creep of Barre granite, Int. J. Rock Mech. Min. Sci., 16, 23-25, 1979.

Kranz, R. L. and C. H. Scholz, Critical dilatant volume of rocks at the onset of tertiary creep, J. Geophys. Res., 82, 4893-4898, 1977.

Ramspott, L. D., L. B. Ballou, R. C. Carlson, D. N. Montan, T. R. Butkovich, J. E. Duncan, W. C. Patrick, D. G. Wilder, W. T. Brough, and M. C. Mayr, Technical Concept for a Test of Geologic Storage of Spent Reactor Fuel in the Climax Granite at the Nevada Test Site, LLNL Report UCRL-52796, 1979.

Sano, O., I. Ito, and M. Terada, Influence of strain rate on dilatancy and strength of Oshima granite under uniaxial compression, J. Geophys. Res., 86, 9299-9311, 1981.

Sprunt, E. S. and W. F. Brace, Direct observation of microcavities in crystalline rocks, Int. J. Rock Mech. Min. Sci., 11, 139-150, 1974.

Tapponnier, P. and W. F. Brace, Development of stress-induced microcracks in Westerly granite, Int. J. Rock Mech. Min. Sci., 13, 103-112, 1976.

Weed, H. C. and W. B. Durham, Drilling-induced borehole-wall damage at Spent Fuel Test-Climax, LLNL Report UCID-19672, 1982.

FIGURE CAPTIONS

1. Crack counting example, BSE/SE pass. a) SEM photomicrograph, scale bar = 100 μm; b) cracks identified as fresh, same magnification as a). There are ten fresh cracks identified here ranging in length from 4 to 104 μm. Mean length here is 24.5 μm. Most of the right half of the picture area is a plagioclase grain. A single quartz grain dominates most of the left half of the picture (lighter contrast). Two other quartz grains are at the upper left and lower right. Note the poorer grain-to-grain contrast as compared to Fig. 2. (Photo ID: 3050/019 Pass A).

2. Crack counting example, BSE pass. a) SEM photomicrograph, scale bar = 100 μm; b) cracks identified as fresh, same magnification as a). There are five fresh cracks identified here ranging in length from 19 to 113 μm with mean length 48.0 μm. The three major phases are, in order of increasing brightness, quartz, plagioclase, and orthoclase. The subtle shadings in the plagioclase probably represent local variations of the Ca/Na ratio within a single grain. The small bright grain at the top was not identified. (Photo ID: 3050/002 Pass C)

3. Low magnification SEM photomicrograph illustrating the heterogeneity of grain sizes in CSDM. Image is BSE only and the scale bar represents 1 mm. The four major contrast levels indicate, in order of increasing

brightness, quartz, plagioclase, orthoclase, and biotite. Small bright spots are various heavier element phases such as iron oxide and zircon. Not shown is the variation in grain size of orthoclase: phenocrysts 100 mm across are not unusual. The grain scale heterogeneity of CSQM may be the principal cause of the noisy crack and strength measurements made on this rock. (Photo ID: 3050/013 Pass B)

TABLE 1: Test Results

Sample	Irradiation Treatment	Stress Treatment	Comments
1	no γ	150 MPa, 60 s; 180 MPa, 60 s; then > 180 MPa	Accidentally overloaded and demolished
2	γ	150 MPa, 60 s; 180 MPa, <60 s	Failed under 180 MPa load
3	no γ	150 MPa, 60 s; 180 MPa, 60 s	No failure
4	γ	150 MPa, 60 s; 180 MPa, 60 s	" "
5	no γ	150 MPa. 60 s	" "
6	γ	"	" "
7	no γ	"	" "
8	γ	"	" "
9	no γ	"	" "
10	γ	"	" "

TABLE 2: Young's Modulus (in GPa)

				----Non-Irradiated------			---------Irradiated--------		
Sample	E_1 (strain < .04 %)	E_2 (strain > .1%)	$\Delta E \equiv E_2 - E_1$	E_1	E_2	ΔE	E_1	E_2	ΔE
1	70.2	70.2	0	70.2	70.2	0			
	64.7	70.7	6.0						
2	54.8	67.5	12.7				54.8	67.5	12.7
	53.1	65.8	12.7						
3	68.7	68.7	0	68.7	68.7	0			
	71.2	74.5	0.3						
4	75.8	77.7	1.9				75.8	77.7	1.9
	76.9	76.9	0						
5	68.2	76.6	8.4	68.2	76.6	8.4			
6	62.4	69.7	7.3				62.4	69.7	7.3
7	61.1	69.4	8.3	61.1	69.4	8.3			
8	63.4	68.9	5.5				63.4	68.9	5.5
9		data not available							
10	54.1	61.3	7.2	___	___	___	54.1	61.3	7.2
	64.3±7.2	70.0±4.9	5.7±4.3	67.1±4.1	71.2±3.6	4.2±4.8	62.1±8.8	69.0±5.9	6.9±3.9

TABLE 3: Crack Statistics by Sample

Sample		# cracks counted	Areal number density (mm^{-2})	Average length (μm)	Areal length density (mm/mm^2)
	(pass B)	18	86	52	4.41
2	(pass A)	31	177	14	2.47
	(pass C)	38	120	30	3.59
		45	157	30	4.70
3		66	206	14	2.79
		20	81	32	2.64
		23	109	36.5	3.98
4		48	171	15	2.54
		51	182	26	4.67
		22	90	41	3.66
5		49	124	14	1.74
		22	75	33	2.46
		12	57	35	1.99
6		64	214	12	2.47
		15	71	44	3.12
		25	119	36	4.27
7		62	158	13	2.07
		30	107	38	4.01
		49	175	28	4.89
8		45	117	15	1.78
		14	67	29	1.95
		34	114	34	3.88
9		46	131	16	2.15
		47	167	23	3.78
		18	86	30	2.53
10		71	285	16	4.44
		35	125	33	4.06

TABLE 4: Crack Statistics by Irradiation/Stress Treatment

	Pass A				Pass B				Pass C				Passes B and C Combined			
	# of Cracks Counted	#/Area (mm^{-2})	$\bar{L}$ (μm)	$\overline{L/Area}$ (mm/mm^2)	# of Cracks Counted	#/Area	$\bar{L}$	$\overline{L/Area}$	# of Cracks Counted	#/Area	$\bar{L}$	$\overline{L/Area}$	# of Cracks Counted	#/Area	$\bar{L}$	$\overline{L/Area}$
180 MPa																
γ	79	173	15	2.51	41	97	43	4.20	89	149	28	4.09	130	128	32	4.14
no γ	66	206	14	2.79	45	157	30	4.70	20	81	32	2.64	65	122	31	3.74
150 MPa																
γ	180	199	14	2.82	79	113	29	3.31	64	91	35	3.15	143	102	32	3.23
no γ	157	134	14	1.92	71	106	37	3.92	96	116	29	3.42	170	112	33	3.64
all																
γ	259	190	14	2.71	120	107	34	3.64	153	118	30	3.58	273	113	32	3.61
no γ	223	149	14	2.11	116	121	34	4.15	119	108	30	3.24	235	115	32	3.64
	BSE/SE pass (Weed and Durham, 1982)													BSE pass		
Sample 2339		105	11	1.13									54	91	36	3.24

TABLE 5: Comparison of Crack Counting Studies

	Rock	Conditions	Confining Pressure (MPa)	# Counted	#/Area (mm^{-2})	L (μm)	L/area (mm/mm^2)
Sprunt & Brace (1974)	Westerly granite	virgin	-	80		3-10[a]	
		$.95\sigma_f$[b]	not given	80		10-30[a]	
Hadley (1976)	Westerly granite	virgin	-	344[c]		1-5[a]	
	" " (T5)	$>.95\sigma_f$	50	632[c]		10-50[a]	
	" " (W5)	failed	150	850[c]		10-50[a]	
Tapponnier and Brace (1976)	Westerly granite	virgin	-	182[d]	196±73[e]		
	" " (T3)	$.58\sigma_f$	50	502[d]	239±48[e]		
	" " (T5)	$>.95\ \sigma_f$	50	861[d]	354±102[e]		
Kranz (1979)	Barre granite	virgin	-	56	7[f]	54±36	
	" "	$.87\sigma_f$, 7s	0.1	262	26[f]	72±42	
	" "	" , 37s	"	282	23[f]	90±79	
	" "	" , 1^5s	"	190	9[f]	146±91	
	" "	" , 136s	"	183	8[f]	164±88	
This study[g]	CSQM	virgin	-	54	91±91	36±47	3.24±3.16
	" , Y	$.92\pm.22\sigma_f$	0.1	143	102±87	32±31	3.23±2.59
	" , no Y	$.73\pm.16\sigma_f$	"	170	112±106	33±30	3.64±3.88
	" , Y	$1.10\pm.22\sigma_f$	"	75	151±137	29±25	4.37±3.90
	" , no Y	$.88\pm.16\sigma_f$	"	65	122±105	31±30	3.74±3.39

Footnotes for Table 4

a median values
b σ_f = failure strength
c includes pores
d cracks encountered in axial traverses not included
e approximated as

$$\text{density} = \frac{\#\text{ of crack intersections along traverse}}{\text{traverse length}} \times \frac{\text{traverse length}}{\text{mm}^2}$$

f approximated as

$$\text{density} = \frac{\#\text{ intersections}}{\text{trace length}} \times \frac{1}{\bar{L}}$$

g BSE data only; Sample 2 (which failed) not included

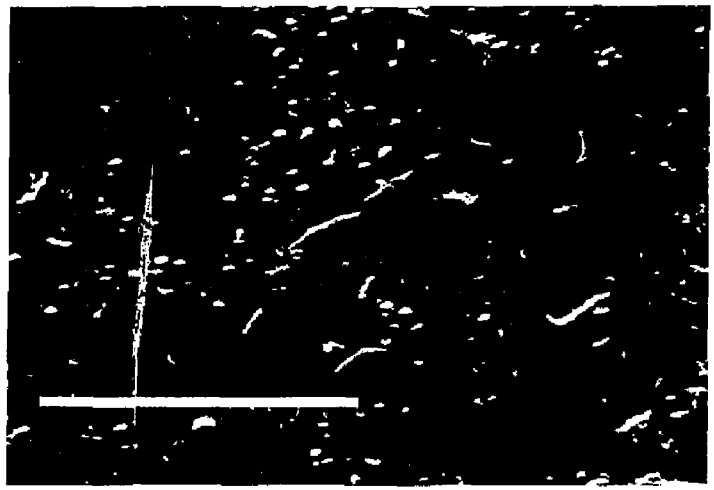

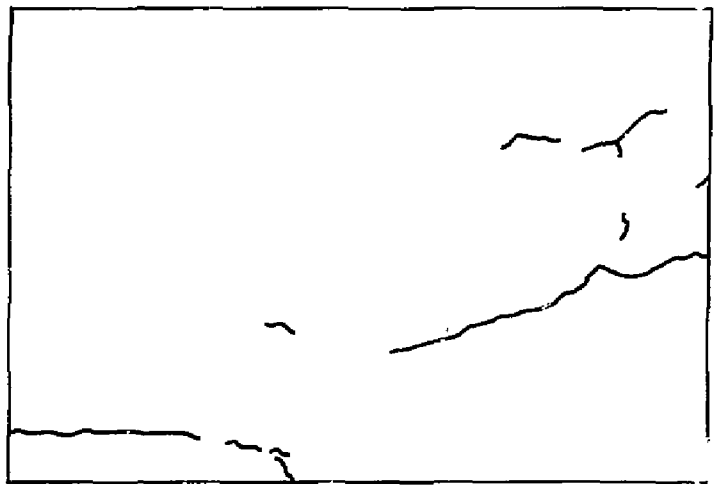

Figure 1

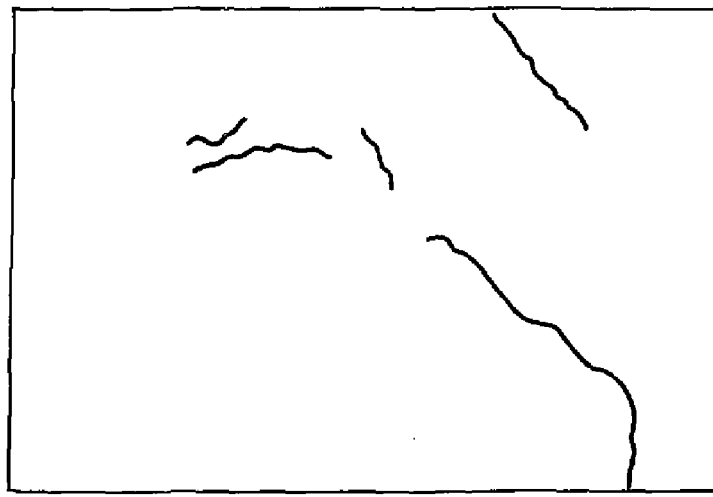

Figure 2

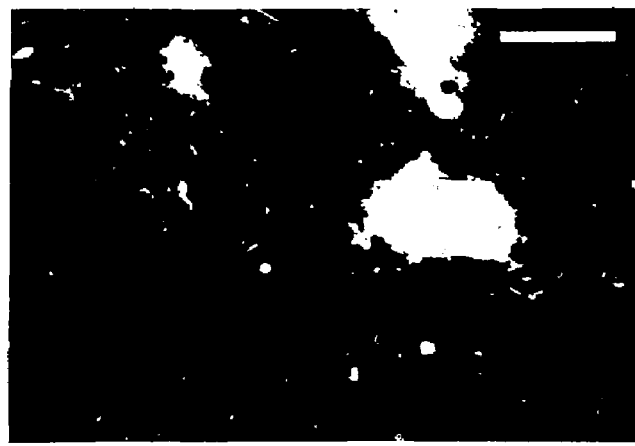

Figure 3